

УДК 620.171.32

V. Gliha¹, P. Maruschak², O. Yasniy², , T. Vuherer¹

¹University of Maribor, Faculty of Mechanical Engineering, Slovenia

²Ternopil Ivan Pul'uj National Technical University, Ukraine

FATIGUE STRENGTH OF WELDS WITH VARIOUS DEFECTS MADE BY VICKERS PYRAMIDE

The summary. The fatigue strength of polycrystalline metals is hardness and defect size dependent. The fatigue strength of welds depends upon the size of grains and actual local mean stress, too. Local mean stress is influenced by the global R-ratio and static preloading. The welds in the as-welded condition are pre-stressed due to the existence of welding residual stresses. The sign and magnitude of residual stresses depend upon the welding conditions. Changes of residual stresses, hardness and defect size were experimentally determined in the present work. Samples of studied metals were prepared by using either thermal cycle simulator or laboratory furnace and water quenching. The methods of microstructure preparation and type of loading result in actual local R-ratio at the used weld toe models. Specimens were cyclic loaded in the similar way like steel at the weld toe. The bottom of the notch was either defects-free or defected by Vickers indentation. Final results show that coarser grain and higher local R-ratios lower the fatigue strength of welds.

Key words: defect size fatigue strength, damageability, heat-affected zone

В. Гліха¹ Ph.D.; П. Марущак² докт. техн. наук, О. Ясній², канд. техн. наук; Т. Вухерер², Ph.D.

ВТОМНА МІЦНІСТЬ ЗВАРНИХ З'ЄДНАНЬ ЗА НАЯВНОСТІ ДЕФЕКТІВ СТВОРЕНИХ ПІРАМІДОЮ ВІКЕРСА

Резюме. Втомна міцність полікристалів залежить від розміру дефекту та твердості матеріалів. Проте, втомна міцність зварних з'єднань залежить також від розміру зерна та локальних напружень матеріалу. Локальні передні напруження визначаються величиною залишкових напружень та параметрами попереднього статичного навантаження. Після формування зварного шва у ньому формуються залишкові напруження знак та величина яких залежать від режиму зварювання. В цій роботі досліджено зміну остаточних напружень твердості та розмірів дефектів у зразках з модельованим термоциклом та після нагрівання в термокамері та наступного гартування. Методи фізичного моделювання структури матеріалу дозволяють відтворити матеріал зони зварного шва. За результатами відтворення експлуатаційного циклічного навантаження виявлено, що збільшення розміру зерна та залишкових напружень в матеріалі знижують втомну міцність зварних швів.

Ключові слова: розмір дефекти, втомна міцність, пошкоджуваність, зона термічного впливу

Introduction. The fatigue damage limits load carrying capacity of welded structures subjected to the variable stress. Material fatigue always results from fluctuating stress. The local fatigue damage is often principal cause of premature failures. The fatigue failures of huge welded constructions are usually catastrophic, leading to severe property damage, environment pollution, and loss of human lives.

Actually, the fatigue damage shortens service life of highly loaded structural components. When the fatigue damage accumulate to an appropriate level, the fatigue crack initiates at the surface of the pre-existing defects usually at stress concentrators such as notches, holes and welds. Once formed, the propagation rate of fatigue cracks is influenced by the load history, micro structure and environmental factors.

A great number of factors affect the behaviour of joints made by welding under cyclic loading as the material strength, weld shape, the sign, magnitude and frequency of stressing as well as the temperature. Processing is not often considered although it determines the homogeneity of weld materials and surface quality as well as the sign and distribution of

welding residual stresses (RS). Thus, the way of processing and particular its metallurgical effects have an overriding influence on the performance of cyclic loaded welded components.

Factors affecting weld fatigue cracking . Typical factors affecting the fatigue cracking of welds are summarised in the following sections: The loading pattern must contain minimum and maximum with large enough variation. The peak stress levels must be of sufficiently high value. If the peak stresses are too low, no crack initiation will occur. The material must be subjected to a large number of stress cycles. One or more properties of the stress state need to be considered, such as stress amplitude, mean stress, biaxiality, in-phase or out-of-phase shear stress, and load sequence. The fatigue strength of anisotropic materials depends on the direction of the principal stress.

The geometry of welds needs to be considered as transitions, notches, variation in cross section and all others that lead to stress concentrations. Because stress raiser in the form of inclusion is not so effective, inclusion fatigue is rare. The surface quality is also important. Roughness cause microscopic stress concentrations that lower fatigue strength. The compressive RS can be introduced in the surface of the most sensitive parts of welds by number of techniques. They produce surface RS in compression which increase the fatigue life of welded component in the case of high-cycle fatigue.

Fatigue life varies widely for different materials. They have specific crystal lattice, strength and fatigue resistance. The high strength steels are much more notch-sensitive than softer steels.

The environmental conditions can cause erosion, corrosion, or gas-phase embrittlement, which all affect fatigue life. Corroded parts form pits which act like notches. Corrosion reduces the amount of material and lowers the strength because it increases the actual stress. The corrosion fatigue is a problem encountered in many aggressive environments. The decarburization is also an important factor because it weakens the surface by making it softer. Stresses due to bending and torsion are the highest at the surface.

Higher temperatures generally decrease the fatigue strength.

Cutting, welding and other manufacturing processes involving heat or plastic deformation can produce high level of tensile RS which decreases the fatigue strength. The RS which add to the design stress may easily exceed the limit stress as imposed in the initial design.

The size and distribution of internal defects as gas porosity, non-metallic inclusions and shrinkage voids can significantly reduce the fatigue strength.

For most metals smaller grains yield longer fatigue lives, however, presence of surface defects or scratches has a greater influence than in a coarse grained alloy.

The results of the present work contribute to understanding how the defect size (DS), grain size (GS) and RS sign and level could affect the fatigue strength of butt-welds.

*Direct influences of welding. **The result of unavoidable thermal treatment during welding is the heat-affected zone (HAZ) and the weld metal (WM) formation.***

Large thermal gradients are consequence of very fast local material heating when welding and pretty fast cooling, too. The reduced ability of solid materials to contract during cooling and especially occurrence of low temperature phase transformation give rise to the appearance of RS in the welds. For this reason some parts of welds can become susceptible to the hydrogen embrittlement and other detrimental phenomena in which RS play an important role. Final results of the RS appearance are various types of weld cracking, distorted joints or simply shorter service life of welded construction.

RS are self-balancing forces. Their character in the most sensitive weld domains to fatigue damage is often tensile. Due to welding some weld domains have totally new or changed microstructure and in such a manner properties. So, those domains can be sensitive to material fatigue and statically tensile pre-stressed. In these spots the conditions for earlier fatigue cracks initiation are advantageous. As well, crack propagation can be faster. The final

consequence is shorter life of welded structure.

Volume weld defects act as the stress raisers while planar defects as the stress intensifications. The effects of the first ones are represented in the experimentally determined and statistically evaluated S-N curves of different types of welds. The effects of cracks have to be evaluated by using fracture mechanics approach, linear-elastic or elastic-plastic depending upon the crack size and stress level.

The resistance of metallic materials to fatigue crack initiation and its propagation depends on the microstructure. Base metals (BM) are chosen with regard to properties, actually due to convenient microstructure. The weakest links of all welded construction are welds, strictly speaking HAZ and WM. The microstructure of both in the as-welded condition is result of the chemical composition and applied welding thermal cycle/cycles.

*Fatigue strength of butt-welds with small defects. **Butt-weld is a weld with the highest effectiveness. In the case of cyclic loading butt-weld cracking is found at the weld toes where stresses are concentrated. If cracks initiated earlier it would be of the greatest importance for the fatigue strength when the conditions for crack propagation are fulfilled, too. The load-carrying capacity of the cyclic loaded welded structures depends therefore upon the actual strength of the most demanded welds.***

Small weld defects as different inclusions, scratches or cracks are often found at the weld toes of butt-welds. Even sharp transitions between weld reinforcement and BM can be treated as small defect. Anyway, the fatigue cracks at the toe of butt-welds initiate often in the coarse-grain material, i.e. the coarse grain HAZ.

Defects decrease fatigue strength of metals because of easier crack initiation. In the past, S-N curves were the only available way to predict the fatigue lives of workshop-quality welds. Now, the LEFM concepts are often applied to the cracks initiation and propagation in metals.

Murakami and co-workers treated the influence of various shaped small defects in the same way as cracks, i.e. using LEFM [1–3]. The parameter reflecting the effect of small defects on the fatigue strength of metals is found to be square root of the defect projection onto the plane perpendicular to the cyclic stress ($\sqrt{\text{area}}$). LEFM underestimates propagation rates of short cracks within the local plastic zones that can develop as a result of stress concentrations in welds [4, 5].

Natural small weld defects in metals can be artificially modelled. As small surface defects drilled small holes are used in the past with success when endurance limit of real quality metals has been studied. Vickers indentation is a promising small artificial surface defect because indenting with the Vickers pyramid is easy to execute. Load on the pyramid has to be adjusted according to the material hardness and the expected indentation size [6, 7].

Problem with use of artificial weld defects is the additional local RS appearance. This kind of RS existence is result of local material plastic deformation when indenting. In order to evaluate only the effects of small defect to the fatigue strength, global RS due processing i.e. welding should be omitted. Electro-etching is usually used to remove surface stratum with the highest RS without any plastic deformation. In such a way, the local and global surface RS are lowered. Unfortunately, the local RS lowering is close linked with the defect's shape and size change. Both influence the parameter of small defect quantified as $\sqrt{\text{area}}$. Global RS can not be lowered separately.

Experimental work and results

Two kinds of CrNiMo steels were used in the experimental work, steels A and B. Chemical compositions are shown in Table 1.

Table 1: Chemical composition of the steels A and B

Steel	C	Si	Mn	P	S	Cr	Ni	Mo	V	Al	Ti	Cu
	<i>mass %</i>											
A	0.09	0.27	0.30	0.015	0.010	1.05	2.63	0.27	0.07	0.045	0.026	-
B	0.18	0.22	0.43	0.012	0.028	1.56	1.48	0.28	-	0.023	-	0.15

The coarse grain microstructure was prepared by simulating thermal conditions in the BM close to the weld on pieces of the steel A in size 15×8.5×70 mm using thermal cycle simulator [8]. Peak temperature of the thermal cycle was at least 1350°C while cooling time $\Delta t_{8/5}$ round 5 and 10 s. The result of simulation was either purely martensitic microstructure or mainly martensitic microstructure with small portion of bainite. Tensile strength, Rm, of materials found at the weld toe and grain size, GS, are shown in Table 2.

Table 2: Tensile strength, grain size and bending fatigue strength at R=+0.02-0.04 of simulated samples made by steel A

Material	Rm	GS	σ_f					
			smooth h	d≅105 μm	d≅160 μm	d≅221 μm	l≅386 μm	l≅692 μm
	<i>MPa</i>	<i>μm</i>	<i>MPa</i>					
HAZ ₁	1210	130	938	915	905	834	-	769
HAZ ₂	1171	140	950	882	-	814	-	769
HAZ ₃	1192	180	927	905	-	814	-	724
HAZ ₄	1176	140	927	927	882	769	-	724
HAZ ₅	1172	180	915	905	-	814	834	724

The bending fatigue strength was experimentally determined on notched specimens in size 14.5×8×70 mm supported at 59 mm. They were machined from samples with simulated microstructure HAZ₁, HAZ₂, HAZ₃, HAZ₄ and HAZ₅ (Table 2). The shape and size of the specimens are shown in Figure 1a. The stress concentration factor caused by the notch in bending is 1.74 [9]. Artificial surface defects of different sizes and shapes were prepared at the bottom of the notch by indenting with a Vickers pyramid. As sketched in Figure 2, they were single indentations of the different size and series of five indentations in line. The average size of single indentations, d, was 105, 160, and 221 μm while the average length of the series, l, 386 and 692 μm. Local RS in the surroundings of the defects caused by indenting were present. Global RS is supposed to be zero because notches were machined after welding thermal cycle simulation.

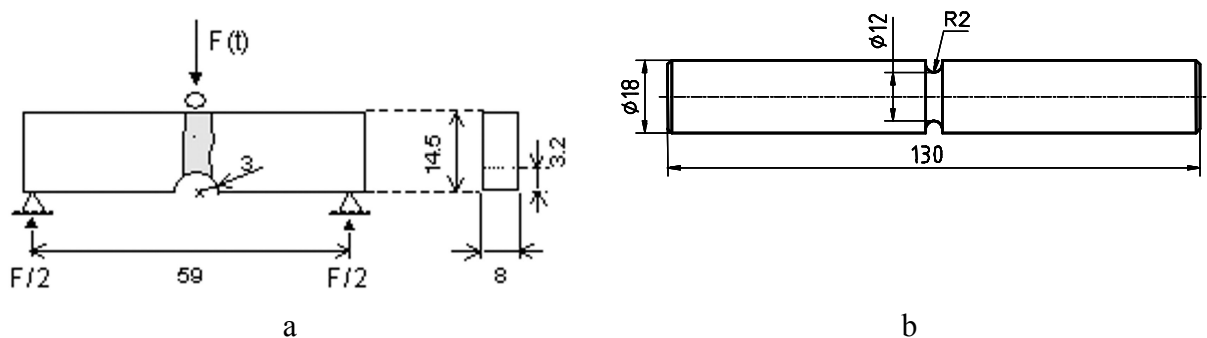


Figure 1. Specimens for fatigue strength determination: The in-plane bending of specimens (a); The rotary bending specimens (b)

Cyclic loading of specimens were executed at the global R-ratio close to zero. All

results of fatigue strength testing, $2\sigma_f$, are shown in Table 2.

The influence of local RS due to indenting with the Vickers pyramid was studied in the next part of the research.

Purely martensitic HAZ_{Simul} microstructure was prepared on pieces of the steel B using thermal cycle simulator and two different heat treatments in furnace. Peak temperature when simulating welding thermal cycle was 1300°C while cooling time $\Delta t_{8/5} \cong 5$ s. The result was coarse grain. The same microstructure was our goal in modelling single-step heat treatment in furnace, namely the coarse grain HAZ_{I-step}. Two-step heat treatment in furnace was modelled for the HAZ_{II-step} simulation. The result of such a simulation was re-refined purely martensitic microstructure formation. Hardness was the same, but grains were much finer [7].

Global compressive RS are result of cylindrical steel pieces water quenching. Their level was assessed by the hole-drilling method round 300 MPa [10]. In contrast to quenching, heat conveying from steel pieces by means of water cooled grips during welding simulation by using weld thermal-cycle simulator results in global tensile RS. We didn't quantify the level of those RS at the bottom of the notch, but they are tensile.

Single Vickers indentations were used as artificial surface defects (Figure 2b). Local RS due to indenting were present in the case when Vickers pyramid was indented after quenching. There were no local RS when Vickers pyramid was indented before quenching local [10]. This was possible only on specimens with microstructure of the HAZ_{II-step}.

Cyclic loading of the specimens with microstructures HAZ_{Simul}, HAZ_{I-step} and HAZ_{II-step} were performed at global R-ratio equal $\square 1$. The results of fatigue strength testing, \square_f , are represented in Table 3. Cyclic loading of the specimens with microstructures HAZ_{II-step} were executed at the R-ratio equal +0.1, too. The results of fatigue strength testing, $2\sigma_f$, are also represented in Table 3.

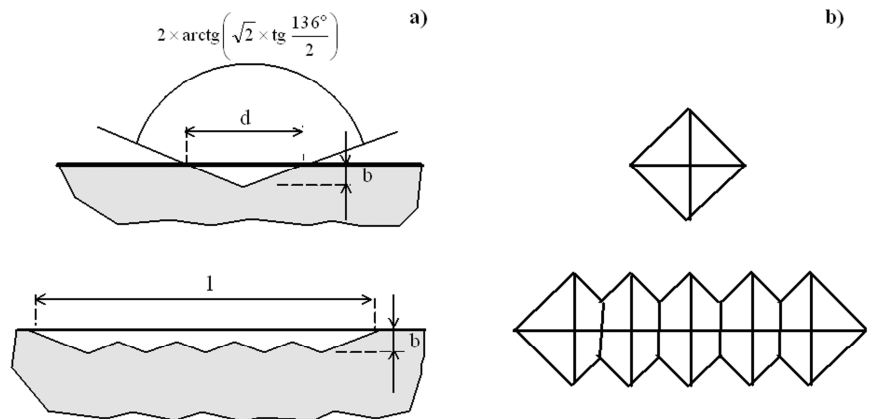


Figure 2: Single and series of Vickers indentations

The bending and tensile fatigue strength was experimentally determined on cylindrical specimens in size 18×130 mm with a little bit different notches in order to have the same stress concentration factor 1.74 [9]. They were machined from the samples with simulated microstructure HAZ_{Simul}, HAZ_{I-step} and HAZ_{II-step}. The shape and size of the specimens are shown in Figure 1b. Artificial surface defects were made by indenting with a Vickers pyramid at the bottom of the notch. The average size of indentations, d , was 200 μm .

Table 3: Tensile strength, hardness, grain size and bending fatigue strength of specimens with the simulated microstructure made by steel B

Material	Rm	Hardness	GS	RS _s	Fatigue strength		
					-	$d \cong 200 \mu\text{m}$ $ RS_1 \geq 0$	$d \cong 200 \mu\text{m}$ $ RS_1 = 0$
	MPa	HV10	μm	MPa		MPa	

HAZ _{Simul}	-	466	200	tensile	σ_f	330	330	-
HAZ _{I-step}	1366	452	200	$\cong \square 300$	σ_f	537	-	-
HAZ _{II-step}	1431	455	20-30	$\cong \square 300$	σ_f	760	664	678
					$2\sigma_f$	1119	998	953

Crack propagation rate was measured on the specimens with the simulated microstructures of purely martensitic HAZs. Resonant testing machine Cracktronic with crack length measuring system Fractomat was used. Threshold stress intensity range for long cracks ΔK_{th} , and constants used in Paris equation C and m were experimentally determined. Their meaning in log-log scale is shown in Figure 3.

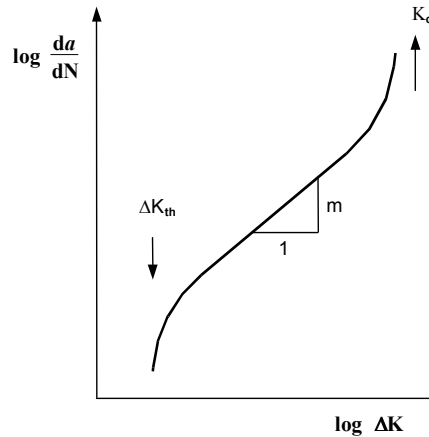


Figure 3. Long fatigue crack propagation rate

Linear part of log-log dependency is so-called Paris equation $\frac{da}{dN} = C(\Delta K)^m$.

Specimens with microstructure HAZ_{Simul}, HAZ_{I-step} and HAZ_{II-step} were tested at R-ratio $\square 1$, whilst specimens with microstructure HAZ_{II-step} at R-ratio +0.1, too. The results are shown in Table 4.

Table 4: Fatigue crack propagation parameters

Material	Rm	Hardness	GS	R	ΔK_{th}	C	m
	MPa	HV10	μm		MPa $m^{1/2}$		
HAZ _{Simul}	-	466	200	~ 1	13	$1.7 \cdot 10^{-13}$	3.6
HAZ _{I-step}	1366	452	200	~ 1	12	$1.7 \cdot 10^{-15}$	4.6
HAZ _{II-step}	1431	455	20-30	~ 1	17	$1.1 \cdot 10^{-13}$	3.5
				+0.1	15	$3.6 \cdot 10^{-13}$	3.2

Discussion. Data from Tables 2 and 3 are shown in Figures 4 and 5. Figure 4a represents the fatigue strength, σ_f , upon the defect size, DS, quantified as $\sqrt{\text{area}}$. We can sketch three simple dependences that correspond to different grain sizes and R-ratios. In general, fatigue strength decreases when defect size increases. The exception are result obtained with very coarse grain and extremely low local R-ratio.

Fatigue strength of polycrystalline metals with small defects is two parameters dependent: $\sigma_f = 1.43 (HV + 120) / (\sqrt{\text{area}})^{\frac{1}{6}}$ [1-3]. The fatigue strength, μ_f , is expressed in MPa, hardness, HV, in Vickers hardness number, and defect size $\sqrt{\text{area}}$ in μm .

Data from Figure 4a are represented in Figure 4b in log-log scale. Only the fatigue strength of specimens with indentations are taken into account. The regression curve that corresponds to medium grain size HAZ materials and local R-ratio close to zero seems to be linear as predicted in Murakami's formula.

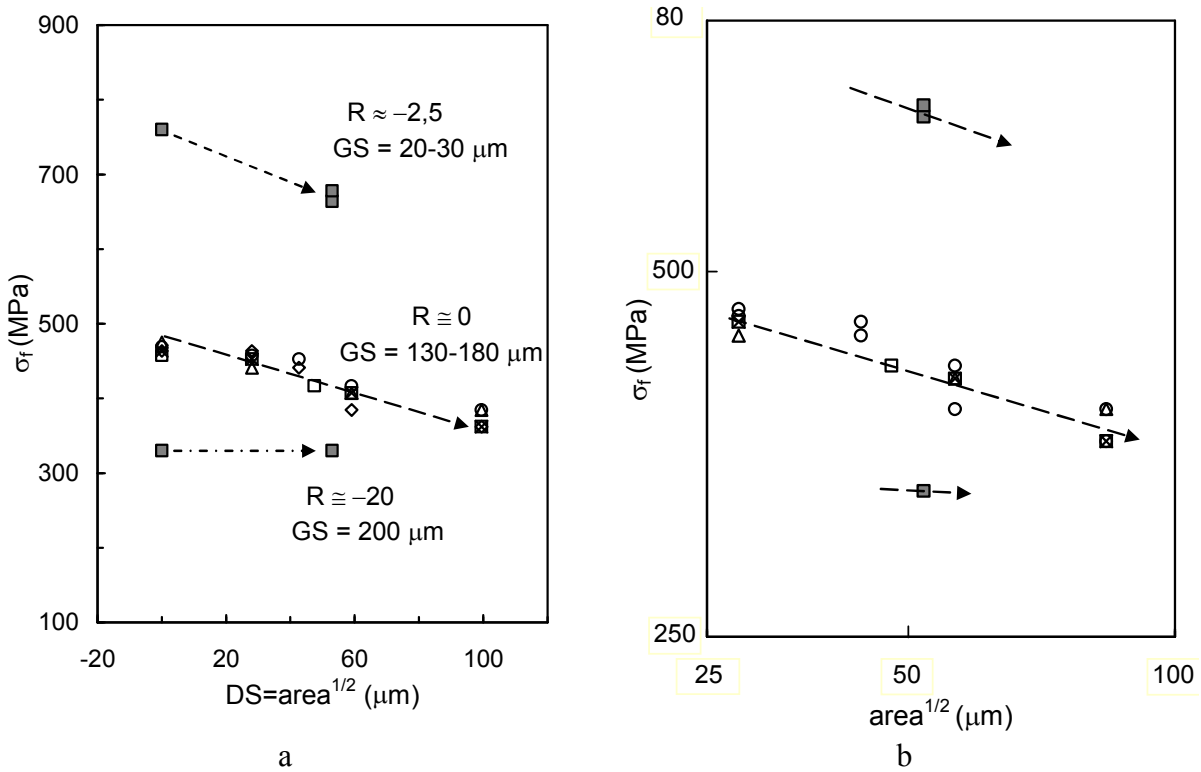


Figure 4: Fatigue strength, σ_f , versus defect size, DS: Linear scale (a); Log-log scale (b)

Obviously, the fatigue strength of polycrystalline steel at the weld toe in welds made in carbon steels is not only two parameters dependent. We see in Figure 4a much different fatigue strength of steels with almost the same hardness round 200 HV and defect size 53 μm . It seems that grain size and global RS level are significant, too. This is of the greatest importance for understanding load carrying capacity of butt-welds under cyclic loading if processing parameters, actually welding parameters, are considered.

Miller [11] pointed out the responsibility of microstructural obstacles for existence of non-propagating cracks at the stress level equal to fatigue strength. The most important obstacles link with the biggest microstructural units of metals are grains, colonies of pearlite in steels with ferritic/pearlitic microstructure, domains with harder microstructural constituent in steels with duplex microstructure, etc.

Considering only distances between grain boundaries, average grain size is crucial. Grain boundaries are more sparsely distributed in space in the coarse grain microstructure than in the fine grain one. This is the reason that once initiated crack that is short can stop to propagate and become a non-propagating crack [11].

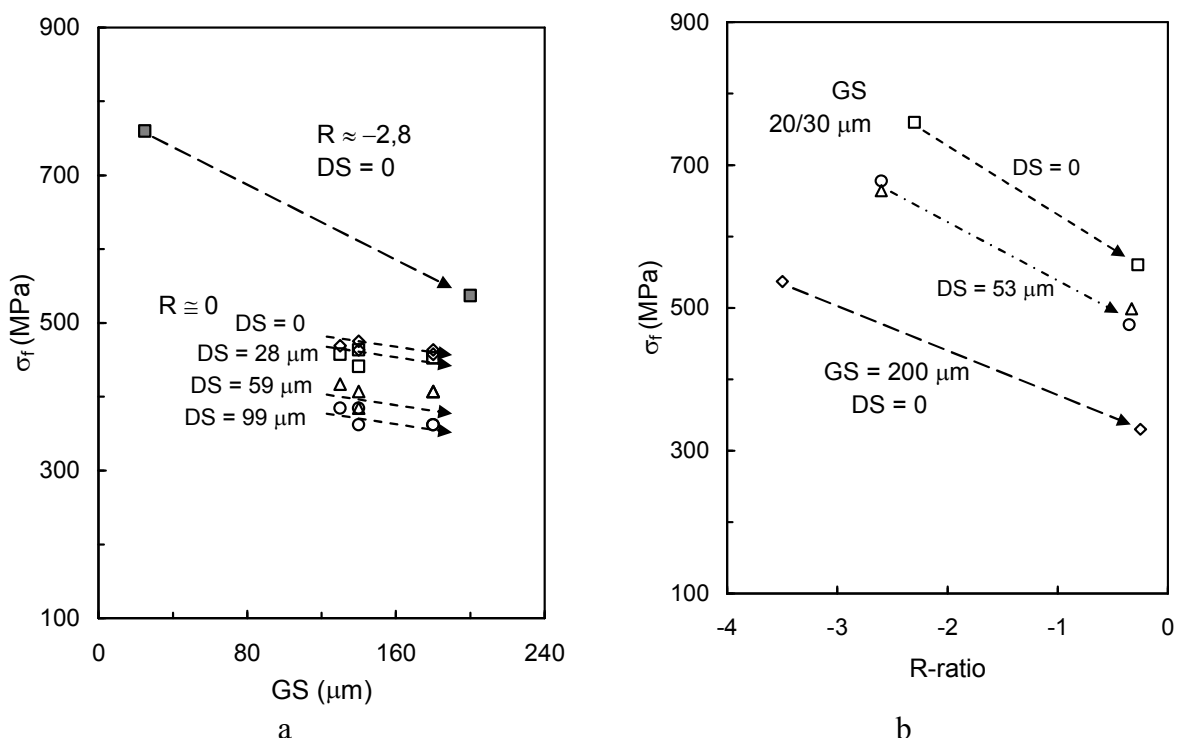


Figure 5. Fatigue strength, σ_f , versus grain size, GS (a) and R-ratio (b) respectively

We can try to explain effects of each variable separately. The dependence of fatigue strength, σ_f , upon the grain size, GS, at two different actual R-ratios that are caused by combination of global R-ratio and effects of RS is shown in Figure 5a. As expected, the fatigue strength decreases with the increasing grain size [6]. The dependence of fatigue strength, σ_f , upon the R-ratio at different grain and defect sizes is shown in Figure 5b. The fatigue strength decreases with the increasing R-ratio like in Smith's and Goodman's diagrams.

Let's talk about experimental data shown in Table 4. Long fatigue crack propagation should be described by using LEFM. In comparison with the properties of the re-fined martensitic microstructure at $R=1$, a lower ΔK_{th} values were registered when coarse grain martensitic microstructures was tested. On the other hand, a lower ΔK_{th} values were registered in re-fined martensitic microstructure at $R=+0.1$ than in case of $R=1$.

In case of coarse grain microstructure with a lower ΔK_{th} value, the fatigue crack that has initiated from small defect can hardly become non-propagating. Cracks start to propagate at lower stress levels. In case of fine grain microstructure with a higher ΔK_{th} value the fatigue crack that has initiated from small defect can become easily non-propagating. Namely, cracks in finer grains start to propagate at significantly higher stress levels.

Higher C and m parameters in Paris equation enable faster long crack to propagation. The result of that is shorter fatigue lives. We can see in Table 4 that lower C-value in the case of both coarse grain microstructures is linked with higher exponent m. The same situation is when we compare the same parameters between coarse and fine grain martensitic microstructures.

References

1. Murakami, Y. at al. Quantitative Evaluation of Effects of Non-Metallic Inclusions on Fatigue Strength of High Strength Steels - I: Basic Fatigue Mechanism and Evaluation of Correlation between the Fatigue Fracture Stress and the Size and Location of Non-Metallic Inclusions, Int. J. of Fatigue, 9, 291-298, 1989
2. Murakami, Y., Usuki, H. Quantitative Evaluation of Effects of Non-Metallic Inclusions on Fatigue Strength of High Strength Steels - II: Fatigue Limit Evaluation Based on Statistics for Extreme Values of Inclusion Size, Int. J. of Fatigue, 9, 299-308, 1989

3. Murakami, Y. Effects of Small Defects and Nonmetallic Inclusions on Fatigue Strength of Metals, *JSME International Journal I*, 32, 2, 167-180, 1989.
4. Gliha, V. Vpliv umetnih površinskih napak na dinamično trdnost materiala na prehodu temena vara. *Mater. tehnol.*, Vol. 35, 1/2, 55-59, 2001.
5. Gliha, V. The effect of small flaws on the fatigue strength of HAZ at the weld toe. *Int. j. mater. prod. technol.*, Vol. 29, 1/4, 297-310, 2007.
6. Gliha, V. Vuherer, T. The Behaviour of Coarse-Grain HAZ Steel with Small Defects during Cyclic loading, *Materials and Technology*, 41, 3, 125-130, 2007
7. Vuherer, T. et al. Fatigue Crack Initiation from Microstructurally Small Vickers Indentations, *Metalurgy*, 46, 4, 237-243, 2007.
8. Gliha, V. The microstructure and properties of materials at the fusion line. *Metalurgija* vol. 44, no. 1, p. 13-18, 2005.
9. Peterson, R.E. *Stress Concentration Factors*, Wiley, 1974
10. Vuherer, T. *Analiza vpliva mikro napak na trdnost pri utrujanju grobozrnatega TVP na varih*, Doktorska disertacija, Maribor, 2008.
11. Miller, K. J. The Behaviour of Short Fatigue Cracks and Their Initiation Part I and Part II, *Fatigue Fract. Engng. Mater. Struct.*, 10, 1, 75-91 and 2, 93-113, 1987.